Exploring Diagnostic Capabilities for Application to New Photovoltaic Technologies

Enrico C. Quintana[1], Michael A. Quintana[1], Kevin D. Rolfe[1], Kyle R. Thompson[1], Peter Hacke[2]

[1]Sandia National Laboratories, Albuquerque, New Mexico, USA
[2]Advent Solar Albuquerque, New Mexico, USA

ABSTRACT

Explosive growth in photovoltaic markets has fueled new creative approaches that promise to cut costs and improve reliability of system components. However, market demands require rapid development of these new and innovative technologies in order to compete with more established products and capture market share. Oftentimes diagnostics that assist in R&D do not exist or have not been applied due to the innovative nature of the proposed products. Some diagnostics such as IR imaging, electroluminescence, light IV, dark IV, x-rays, and ultrasound have been employed in the past and continue to serve in development of new products, however, innovative products with new materials, unique geometries, and previously unused manufacturing processes require additional or improved test capabilities. This fast-track product development cycle requires diagnostic capabilities to provide the information that confirms the integrity of manufacturing techniques and provides the feedback that can spawn confidence in process control, reliability and performance. This paper explores the use of digital radiography and computed tomography (CT) with other diagnostics to support photovoltaic R&D and manufacturing applications.

INTRODUCTION

Exponential market growth and potential for economic gain has recently fueled unparalleled technological creativity that is challenging traditional photovoltaic components designs and their manufacture. These challenges further demand that researchers provide the diagnostic capabilities that support R&D as well as validate the characteristics of these new technologies. This paper looks at these increasing needs and highlights diagnostic capabilities being evaluated for application in photovoltaics.

For the most part, photovoltaic modules, predominantly crystalline silicon, have been manufactured the same way for that past 25 years. Recent materials, manufacturing and market advances have driven down costs, rapidly approaching an asymptote. Today, we are witnessing challenges to the way that conventional crystalline silicon modules are made, including materials, designs, and manufacturing processes. Additionally, the emergence of new technologies (CdTe, CIGS, a-Si, OPV, and CPV) are challenging the dominance of crystalline silicon in the marketplace with totally different materials, designs, and manufacturing processes. In parallel, the commercial sector has undertaken a two-pronged approach at improving BOS equipment. Development of more sophisticated and more cost effective BOS components is leading to enhanced system features using new components, new designs, new materials and even departures from conventional central inverter approaches that have so dominated system designs. Needs for enhanced communications, data collection, system diagnostics, greater reliability, and greater suitability to diverse environments is spawning development that makes a system much more than the array and inverter of yester-year.

DIAGNOSTIC MEASUREMENTS

Advancement of a technology depends wholly on the ability to characterize those attributes which can ultimately lead to useful applications in the marketplace as well as produce opportunity for growth and profit. In the symbiotic relationship between photovoltaic researchers and the marketplace, we see a demand, a desire, for clean solar energy as well as an increasing demand for data, information, and assurances that photovoltaics can perform as promised and take its place within a complex and diverse stable of energy providers.

In a broad compilation of diagnostic measurements, also referred to as characterization techniques, Kazmerski, listed twelve categories of properties of photovoltaics along with characterization techniques that are too numerous to mention.[1] This compilation published in 1998 reflects an industry still in its infancy with many of the techniques focused on device characterization in the fundamental R&D phase. All of these techniques remain relevant today but a continually increasing need has emerged: accurate and fast techniques that provide information needed by manufacturers wishing to get products to market quickly. Oftentimes the need(s) are amplified as manufacturers attempt to pass the crucial qualification/certification tests specified by IEC and/or UL standards and the focus is packaging. Diagnostic needs are also driven by heightened awareness of reliability and distinctively different geometries and designs.

Recently we have had opportunities to exercise CT in combination with other diagnostics to assist partners in the photovoltaic community. Additional ideas are being triggered about how these and other diagnostics might be used as manufacturers continue to develop

new technologies. This paper discusses this work and potential for continuation.

CT TEST TECHNIQUE

Computed Tomography (CT) is an extremely powerful diagnostic tool. Originally developed for the medical field, CT has become a common part of industrial nondestructive testing (NDT). Industrial CT systems provide information about internal material characteristics of objects being examined. The basic geometry of a CT system has a collimated point source of x-rays, a rotary stage that holds the component to be inspected, and a two-dimensional x-ray imaging detector. The spatial relationships between each of these features are critical. The relative positions of each part of the CT system must be known to a degree commensurate with the desired output spatial resolution. The output from traditional x-ray imaging integrates 3 dimensional part geometries into 2 dimensional space. CT allows a 3 dimensional part to be represented in 3 dimensional space by reconstructing thin cross sectional slices of the part based on a series of x-ray images.

While there are several different generations of CT, cone beam CT is the primary focus of this paper. As illustrated in figure 1, cone beam CT consists of an x-ray source with a cone shaped X-ray beam and a flat panel 2-dimensional detector.

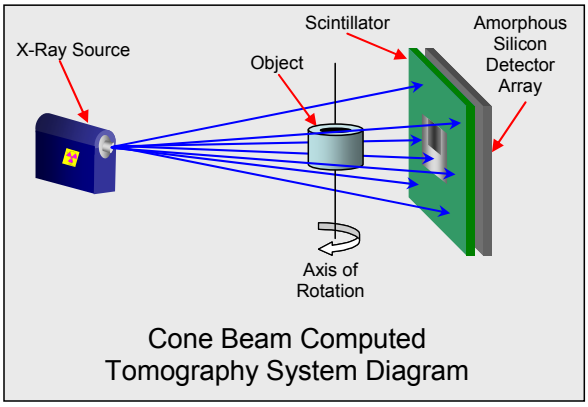

Figure 1 Diagram depicts Sandia's Cone Beam CT scanning system

CT spatial resolution is primarily determined by two factors: x-ray focal spot size and detector pixel pitch. Typically with industrial CT, parts are placed as close to the detector as possible, as the limiting factor being is typically the focal spot size of an x-ray source (a few mm's) when compared to the detector pitch (less than 1 mm.) Micro CT utilizes geometric magnification to allow for higher spatial resolution. When performing Micro CT, the component being inspected is placed closer to a micro-focus x-ray source, essentially casting a larger shadow onto the detector. This is the same concept as changing the size of the shadow of an object in front of a flash light by moving the object closer and farther from the flash light. The micro focus x-ray source has a variable focal spot size which is a function of the power output and can range from 1-100 µm. The magnification is defined as:

$$Magnification = \frac{STD}{STP}$$

Where STD is the source to detector distance and STP is the source to part distance. Placing an object half way between the x-ray source and detector results in a 2x magnification.

The focal spot size can then be determined by:

$$Spot\ Size = \frac{Detector\ resolution}{Magnification}$$

The x-ray machine is operated at a focal spot size at or below the value determined from the equations above. Operating above this value will result in loss of image sharpness and thus, lower spatial resolution.

From these equations it is easy to see that the effective resolution is very part dependent. Smaller parts will allow for higher resolution scans because the part can be positioned closer to the source. At Sandia, an amorphous silicon x-ray detector is used for Micro CT and has a detector resolution (pixel pitch) of 127 µm with an active area that is 25 cm in width by 20 cm tall.

Once the part is positioned, x-ray images are acquired at various positions as the part is rotated through 360°. The x-ray image acquired at each of these rotary positions is called a projection image. Ideally, the number of projections acquired for a CT scan is determined by the number of horizontal pixels in the x-ray image. The ideal number of projections is $\Pi/2$ times the number of horizontal pixels in the projection image. The number of projections can vary from a few hundred projections to thousands of projections. Fewer projections can be used at the cost of CT image quality. A typical scan can last from a few minutes to hours.

These projection images form the basis for the reconstruction. This process is computationally intensive involving computer systems with 20-30 processors. Reconstruction takes the same horizontal line in each projection and reconstructs them into a single slice. Therefore, the number of slices corresponds to the number of pixels in the direction orthogonal to the axis of rotation (number of vertical pixels in the projections.) Several commercial software packages are then used to stack the images, re-slice different views, and create 3-dimensional representations. [2, 3]

Examples of recent work

Figure 1 shows the photographic and CT images of a CPV prototype cell assembly. The first image shows the construction of a typical cell assembly. A critical interface for both electrical conduction and thermal management is shown next. The CT scan of the assembly showed slight geometric variation at the perimeter and some porosity but no major voiding that would be cause for concern, especially for efficient heat transfer to the substrate.

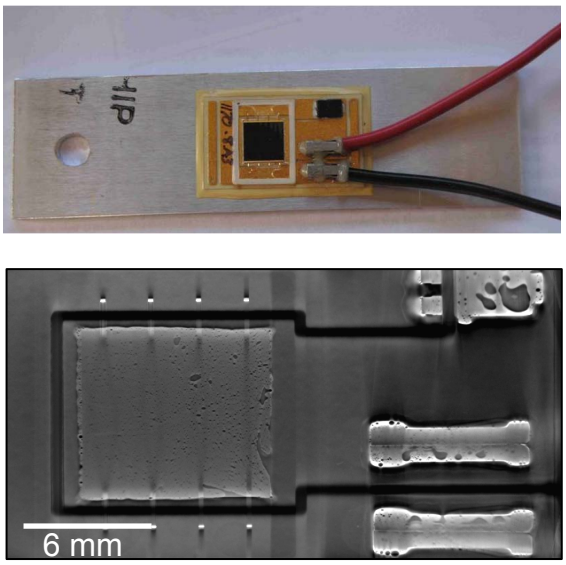

Figure 1. CPV cell assembly and a CT scan imaging showing the interface material between the cell and the substrate. (25 µm resolution)

In Figure 2 and Figure 3 we show images from a completely packaged electronic component generated with CT. The objective of the CT scan was to examine the packaging for voids in the multi-functional potting. The emphasis was to assess potential effects on thermal management and to search for possible reliability issues. One such issue could be voids that bridge electrical contacts with a high potential difference. If these voids subsequently absorb moisture, a potential for shorting and a failure could occur.

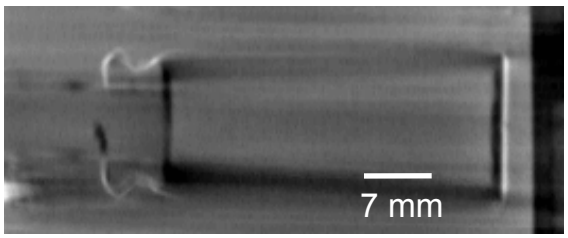

Figure 2 shows a capacitor with large void between leads.

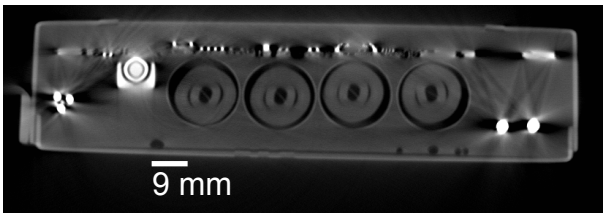

Figure 3 CT shows additional voids in the potting (Note the resolution of the components at the top of package)

ULTRASONIC TESTING

Ultrasonic testing relies on mechanical waves or vibrations and their propagation in solids. Ultrasonic waves begin at a frequency of 20,000 Hz and typical ultrasonic testing utilizes frequencies above 10 MHz. The physical property of a material, (i.e. acoustic impedance) determines the velocity at which sound waves will propagate.

Sound waves are both transmitted and reflected at each interface between two materials with dissimilar acoustic impedances. The transmitted wave continues through the material until it reaches another interface, where again, it is split into transmitted and reflected waves. Thus the amplitude of the transmitted wave is reduced at each interface. This continues at each interface creating sound waves in both directions throughout the material. The amplitude of the signal and the time it takes to reach the receiver provides information on the part being inspected. If a void or disbond exists at any interface, a greater proportion of the sound wave will be reflected. [4]

CASE STUDY USING MULTIPLE DIAGNOSTICS

Advent Solar has introduced Ventura, an integrated module architecture for the emitter wrap-through (EWT) cell. The EWT cell is based on p-type multcrystalline Si which has the phosphorus-diffused emitter wrapped to the rear of the cell by means of micro through-holes.[5] As a back contact cell, both positive and negative grid fingers and contacts are on the cell rear. Higher conversion efficiency and better aesthetics result from the removal of the front grid lines and closer cell packing can be achieved in the module as well. Using proven semiconductor-style manufacturing techniques, Monolithic Module Assembly (MMA) technology enables fully automated module assembly for the first time, delivering scalable high volume module manufacturing capabilities. MMA also allows EWT cells to be used in an optimal way by reducing series resistance losses within cells and at the module level [6, 7].

A single step lamination process of placing back contact cells using an electrical conductive adhesive (ECA) or low temperature solder has been described previously [8]; see Figure 4. In one manifestation, back contacted cells are connected by means of an ECA to a foil etched into an appropriate circuit design to

interconnect cells into a string. A dielectric layer is patterned on top of the foil to insulate it from gridlines of opposite polarity of the cell; this functions as an inter-layer dielectric (ILD). The foil is backed by a support layer such as polyethylene terephthalate (PET) and an environmental barrier layer such as polyvinyl fluoride PVF. The cell is encapsulated and bound to the back sheet and glass by a suitable encapsulant such as ethylene vinyl acetate (EVA). The encapsulant and the electrical bond (solder or ECA) are reflowed and cured simultaneously in the monolithic module assembly process.

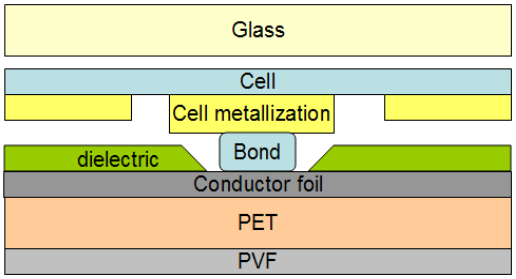

Figure 4. Cross section of the backsheet, conductor foil, bond, and cell structure assembled in a single laminator step to encapsulate and achieve the electrical bonds. *Adapted from P. C. de Jong et al. Proceedings of the 19th EPVSEC, Paris, June 7-11 2004, p. 2145*

Highly reliable MMA module packages designed to last more than thirty years in the field are built with the assistance of improved diagnostics. These diagnostics also enable quick development of new and reliable materials and designs. This section describes results of such diagnostics that assist with failure analysis in the development stage and quality assurance of the product.

In the diagnostic process, regions of interest are first determined by conventional infrared imaging techniques. Hot or cold spots are identified and their nature (shunt path, resistive, open circuit) is hypothesized based on the exhibited electrical properties and the images. These locations are imaged and examined in more detail with CT and ultrasound C-scans. We show how CT can image defective joints, shunt paths, and voids in the electrically conductive bond between the cell and the foil backsheet. Ultrasound C-scans, on the other hand, can image electrically conductive bonds that have separated (known as kissing disbonds) and other interfaces that have delaminated.

Characterization of shunts by CT

Far-infrared imagining techniques can be used to locate shunt paths and abnormally high series resistance (Figure 5). Such imaging techniques can be used to identify problems with photovoltaic modules; however, the nature of the conductive path causing Joule heating may not be visible to the eye, such as a path that originates from a defect existing between the active cell and the backsheet.

When a string of solar cells in a module is forward biased, current generally flows evenly through the forward biased p-n junction of the cells, but in the case of a shunt, where metallization of one polarity is in direct contact with metallization of the opposite polarity, for example, current will preferentially flow through that connection leading to localized heating.[9] Back contact cells have metallization of both polarities on the rear face with different opportunities for shunting. Cell metallization is generally isolated from the backsheet foil by a polymer ILD, a failure of which leads to shunting. Materials used for the electrically conductive bond between the cell and the backsheet also have the potential to short positive and negative polarity gridlines if applied improperly.

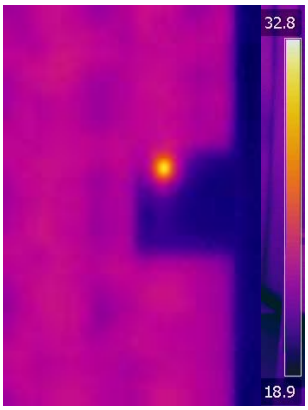

Figure 5. Far-infrared image of a shunt in a module with 8.5 A forward bias; temperature scale is given in (ºC).

In Figure 5, a cell is shown to be essentially dark (cold), with the exception of a region in the upper left hand corner of that cell which appears as a hot spot. Based on this image, the current passing through that cell is judged to be concentrated at that location, a shunt. As seen in the adjacent cells, current is normally evenly distributed through the entire diode region of the cell, leading to a more uniform temperature distribution.

Further examining the localized heating (hot spot) by far infrared imaging in Figure 5, a plan view X-ray of the interconnect (not shown) did not reveal any smearing of the interconnect between regions of opposite polarity, but a CT scan in cross-section of the region indicated severe deflection of the backsheet foil into the plane of the cell's gridline metallization (Figure 6). Cell gridlines are perpendicular to the page, seen as white points, with the foil layer just above. At region **a**, the backsheet foil is observed to be pressed down against the gridlines at a shunt point, the origin of the hot spot on this cell. A cross section of a small portion

of the electrical bond connecting the back sheet foil (above) to the bond pad on the cell (below) can be seen at **b**, revealing the presence of a void. At region **c**, the back-sheet conductor foil is satisfactorily separated from the cell gridlines by the ILD, which is not contrasted by the X-ray CT.

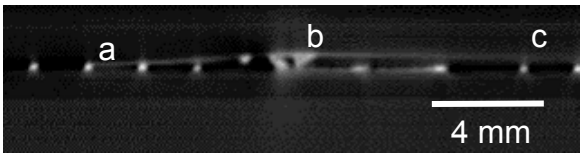

Figure 6. Shunted area seen in cross-section by CT (30 µm resolution)

CT scans also indicate bowing of the backsheet foil toward the cell metallization at the edge of the module associated with encapsulant pinch-off, whereby the fluidized encapsulant escapes at the edges of the module during lamination (Figure 8).

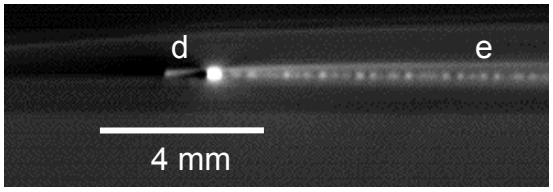

Figure 8. CT image of the edge of the module. (30 um resolution)

At **d**, the encapsulant is pinched off, resulting in the pressing of the backsheet foil into the busbar of the cell, which is normal to the plane of the image and seen as a strong white point. The backsheet foil can shunt with busbars of the opposite polarity by this mechanism. At **e**, separation is acceptably maintained between the backsheet foil and the Ag gridline below. As the backsheet material, including the foil, is driven toward the cell metallization, the likelihood of shunting is increased. This shunt mechanism can fortunately be eliminated with proper precautions during the module assembly process and through robustness of the module design.

Series resistance root-cause analysis by electroluminescence and ultrasonic C-scans

Stresses associated with accelerated lifetime testing have indicated potential failures in ECA bonds in some back contact cell and backsheet designs.[10] In this work, electroluminescence (EL) was used to image a twelve cell mini prototype module that was exposed to accelerated damp-heat and humidity- freeze testing. EL indicates regions of significantly higher series resistance around the cell edges (Figure 9).[11] A calculated increase in series resistance associated with the environmental stress of 0.63 Ω-cm^2 was determined by module testing with a sun simulator.

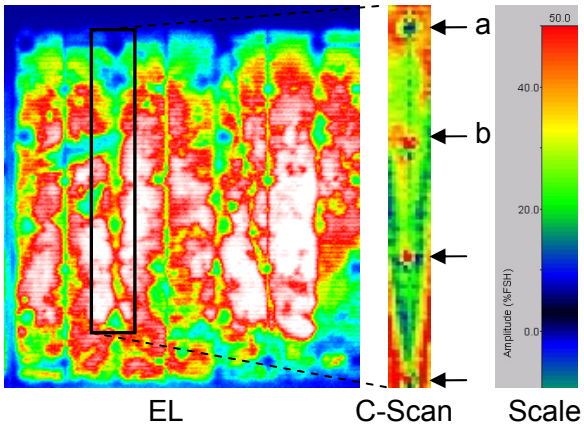

Figure 9 - EL image of a cell and a C-scan image of a section shows correlation of series resistance and lack of bond. Blue indicates regions of high series resistance in the EL image, and delamination or disbonding in the C-scan image.

Ultrasound C-scans were used to non-destructively test the condition of the prototype module. Two forms of immersion ultrasonic testing methods were employed to evaluate the ECA bonds in the cells, Pulse Echo (PE) and Through Transmission Ultrasound (TTU), the latter being the more successful. In immersion testing (Figure 10) both the ultrasonic transducer and the part being inspected are submerged into de-ionized water, which facilitates the transmission of the ultrasonic sound waves into the part. In TTU mode, two transducers are used on either side of the specimen; one to pulse and another to receive the sound wave. In this mode the sound travels in one direction and allows inspection of the entire thickness of the part.

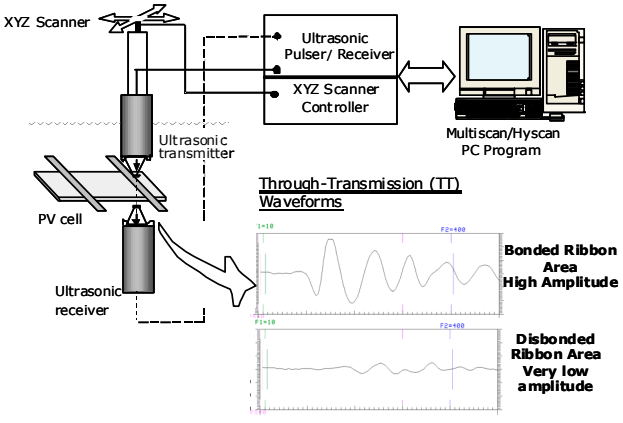

Figure 10 – Set-up for TTU inspection

The part was scanned and indexed along two axes at 0.050" increments while positive and negative amplitude was collected at a frequency of 250 MHz. Assembly and analysis of the data produced the C-scan image of the part as seen in Figure 12.

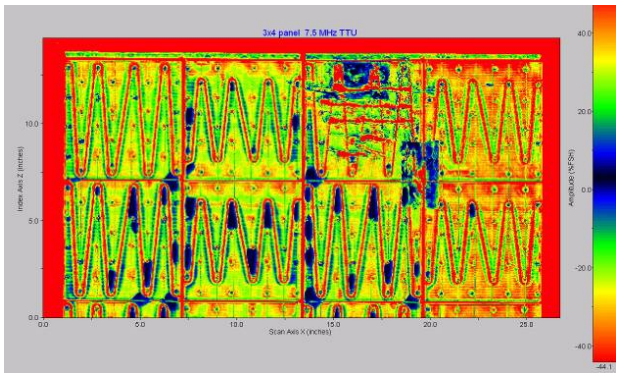

Figure 12 – Ultrasonic C-Scan image. Red represents the absolute maximum signal amplitude, both positive and negative values, and indicates areas where good bonds exist. Blue represents little to no signal amplitude indicating areas with poor bonding.

A region of the C-scan with special focus on the bonds is shown on the right hand side in Figure 9. A correlation is made between the EL image on left, indicating variation in series resistance of a region of a prototype EWT-MMA module that has been stressed through accelerated lifetime testing and a portion of the C-scan image. Examining the bonds, we see regions of high resistivity in the EL image, primarily at the perimeter, correlating with high attenuation of C-scan signals, indicating disbonds. White and blue regions in the EL image correspond to regions of low and high series resistance respectively. The C-scan image of a specified region covering four interconnects (indicated by arrows) to the backsheet foil is shown on the right. It is seen that areas of low resistivity in the cell (white/red in the EL image) show no discontinuities in the nearby interconnects (red points, **b**), whereby the interconnect at the top is dark blue because of strong attenuation of the acoustic signal, indicating a disbond, **a**.

The observations were confirmed in several instances by cutting into the backsheet and testing electrical continuity over the bond. Ultrasound is therefore a tool that can be used for root cause analysis, identifying separation of interconnect bonds that lead to increased series resistance and lower module power. The combination of capabilities, EL and C-scan, has lead to a successful diagnosis and corrective actions.

RESULTS

Diagnostic tools are key to R&D of new photovoltaic products. Non-destructive testing is especially valuable for quick diagnostic studies as products approach commercial introduction. Results show how advanced Computed Tomography (CT) is being introduced to PV R&D and how CT might be used for validation of manufacturing processes and for reliability studies, including failure analyses. New photovoltaic module geometries, materials, and construction approaches, as well as lingering reliability issues such as µ-cracks in Si cells, will be the focus of future studies Sandia National Laboratories has conducted several tests on proprietary components with highly positive results and will continue to develop this capability in support of the Department of Energy's Photovoltaic Program.

ACKNOWLEDGEMENTS

Sandia is a multiprogram laboratory operated by Sandia Corporation, a Lockheed Martin Company, for the United States Department of Energy's National Nuclear Security Administration under contract DE-AC04-94AL85000. Sandia acknowledges the support of the DOE Solar Energy Technologies Program in particular for the work presented here.

REFERENCES

[1] L. Kazmerski, "Photovoltaics characterization: A survey of diagnostic measurements", *Journal of Materials Research,* vol 13, no 10, 1998, p. 2684.
[2] J. Hsieh, *Computed Tomography: Principles, Design, Artifacts, and Recent Advances*. Bellingham, Washington: SPIE Press, 2003.
[3] T. M. Buzug, *Computed Tomography: From Photon Statistics to Modern Cone-Beam CT*. Berlin: Springer-Verlag, 2008.
[4] J. Krautkrämer and H. Krautkrämer, *Ultrasonic Testing of Materials*. Berlin: Springer-Verlag, 1990.
[5] J. M. Gee, W. K. Schubert, and P. A. Basore, "Emitter Wrap-Through Solar Cell", *23rd IEEE PVSC*, 1993, p. 265.
[6] P. Hacke, et. al. "Optimized Emitter Wrap-Through Cells for Monolithic Module Assembly", this conference.
[7] J. Gee, et. al. "Development of Commercial-scale Photovoltaic Modules using Monolithic Module Assembly", this conference
[8] P.C. de Jong et al., " Single-step laminated full-size. PV modules made with back-contacted MC-Si cells and conductive adhesives", *19th EPVSEC*, 2004, p. 2145.
[9] S. A. Correia et al., "Eliminating Shunts from Industrial Silicon Solar Cells by Spatially Resolved Analysis", *19th EPVSEC,* 2004, p. 1297.
[10] P.C. de Jong, et. al. "Progress Made with Back-Contact Modules Using Conductive Adhesive Interconnection Technology", *22nd EPVSEC*, 2007, p. 2679.
[11] Y. Takahashi et al., "Luminoscopy - Novel Tool for the Diagnosis of Crystalline Silicon Cells Utilizing Electroluminescence", *IEEE 4th World Conference on Photovoltaic Energy Conversion*, 2006, p. 924.